Scientific
Research
Publishing

Optimization of the Angle of Frog in Mouldboard Tillage Operations in Sandy Clay Soil

Angela Hiuhu*, Ayub Njoroge Gitau, Duncan Onyango Mbuge, John Ndisya Mulwa

Department of Biosystems Engineering, University of Nairobi, Nairobi, Kenya
Email: *angela.hiuhu@gmail.com, gitauan@yahoo.co.uk, mulwa88@gmail.com

Abstract

This paper investigated the effect of three independent variables including: tillage speed (ranges of below 2.5 m/s and between 2.5 m/s and 5 m/s), tillage depth (range of 10 cm from 0 cm to 30 cm) and frog angle (30°, 40°, and 50°) on draught forces. The experimental work was completed with determination of the draught forces using an analytical method (Saunders Equation). Numerical Simulation: Discrete Element Method (DEM) was used to verify the results obtained analytically. The results indicated that tillage depth has a stronger influence on the draught forces as compared to the tillage speed. Minimal draught forces can then be achieved through operating at shallow tillage depth and maintaining a frog angle of 30°. The results showed a variance of ±15.95% to the calculated values supporting DEM as a numerical method capable of predicting draft forces correctly, tillage power optimization and determination of optimal frog angle for the mouldboard plough.

1. Introduction

Tillage is a necessary action on soil to prepare favorable conditions for plant growth however, it is costly and time consuming [1]. In soil tilth preparation, primary tillage is considered as the largest power consumer operation [2]. For this reason tillage power optimization is still one of the main research fields [3]. Research has been carried out to optimize performance of soil implements and reduction of tillage power through various methods:

---

*Corresponding author.

optimization of tool geometry [4]-[6] and strip tillage [7]. Accurate modelling is necessary for the design of energy efficient soil implements in different operating conditions [8]. Draught force of a mouldboard plough is dependent on the plough geometry, soil properties and operation factors (cutting speed and depth) [5].

Soil-cut interactions have been studied experimentally and analytically [5] [9]. Empirical formulas are also used to study soil-cut interactions however they are limited to relatively simple geometries of the working tool [10]. With the advancements in computer science, numerical methods are now used to predict draught forces. Numerical methods are further divided into [11]: Finite Element Model (FEM), Computational Fluid Dynamics (CFD) and Discrete Element Model (DEM). This study used DEM model as it considers soil failure, deformation and can handle large particle displacement.

[12] developed DEM for the study of rock mechanics. DEM describes mechanical behavior of granular materials through the study of the contact forces between finite number particles and their interactions hence suitable for modelling soil-cut interactions [13]. DEM allows for creation and breakage of contact between elements and the study of formation of cracks propagation involved in the field operation of a soil engaging implement. It also allows for the study of the relationship between micro and macro behavior. DEM has been in use in the past for various applications: [11] [14]-[18]. The objective of this paper is to optimize the design parameters of the mouldboard plough and in particular the frog angle. Altering the frog angle affects how the soil is cut and inverted impacting the draught forces. Numerical formula (DEM) was used and the results were compared to the analytical formula (Saunders Equation).

In contrast to the analytical formulas, use of DEM allows for the prediction of draught forces for complex tool geometrics hence optimizing performance for the mouldboard ploughs.

2. Development of Soil Interaction Model

2.1. EDEM™ Model

EDEM^{TM} is a modeling platform in-built in DEM. It is based on the Hertz Mindlin contact force model and in particular the parallel particle bond model as shown in **Figure 1**. Equations (1) and (2) show the governing equations of the model.

$$F_i = F_n n_i + F_s t_i \tag{1}$$

$$M_i = M_n n_i + M_s t_i \tag{2}$$

The contact forces, normal force (F_n^s) and tangential force (F_t^s) shown in Equations (1) and (2) between particles are computed using the Hertz Mindlin contact law. A damping force is added to the normal damping force (f_n^d) and the tangential damping force (f_t^d) to show the viscous behavior. The contact forces are defined as functions of the normal and tangential stiffness (K_n and K_t), normal and tangential relative displacements. While the damping forces are determined as functions of the damping coefficient and the relative velocity as per [19], the friction is well modeled using the Coulomb's law of friction.
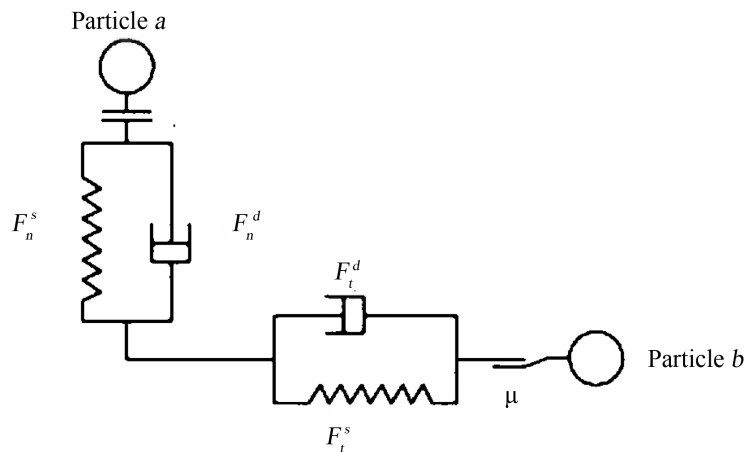

Figure 1. Schematic representation of the contacts.

Table 1 shows the global settings of the EDEM^{TM}, the units and values of the different parameters. These parameters are found in the main window and are kept constant for all the iterations of simulation performed [20].

2.2. Particle Modelling

The soil particles were remodeled in EDEM using optimal imaging techniques as shown in the below images. **Figure 2** shows a pictorial representation of soil while **Figure 3** shows the simulated soil particle.

A virtual soil bin was created using the EDEM as shown in **Figure 4**. The particles filled the soil bin at a rate of 3000 particles per second until the bin filled. The particles were set to be distributed in a log-normal manner and were placed randomly in the bin at a velocity of 20 m/s. the time step was set at 15 seconds with a time interval of 0.1 seconds as per **Figure 5**.

EDEM^{TM} was calibrated using the angle of repose. Values of surface energy, coefficient of restitution, coefficient of static friction and coefficient of rolling were adjusted iteratively until the value of the angle of repose in simulation was close to the experimental value. **Figure 6** shows how the angle of repose was measured in simulation. Macro mechanical strength parameters were determined using the standard tests e.g. the shear test.

Table 1. Global EDEM^{TM} settings.

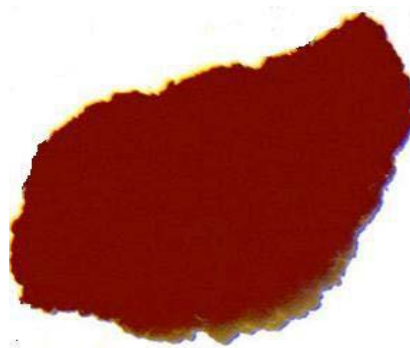| Property	Units	Value
Gravity	m/s^2	−9.81
Poisson's Ratio of Steel	No units	0.3
Shear Modulus of Steel	Pascal	7×10^{10}
Density of Steel	Kg/m^3	7850
Poisson's Ratio of Soil	No units	0.25
Shear Modulus of Soil	Pascal	1×10^{10}
Density of Soil	Kg/m^3	1818

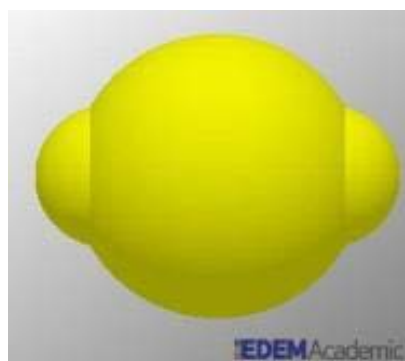**Figure 2.** Soil particles to be remodeled.

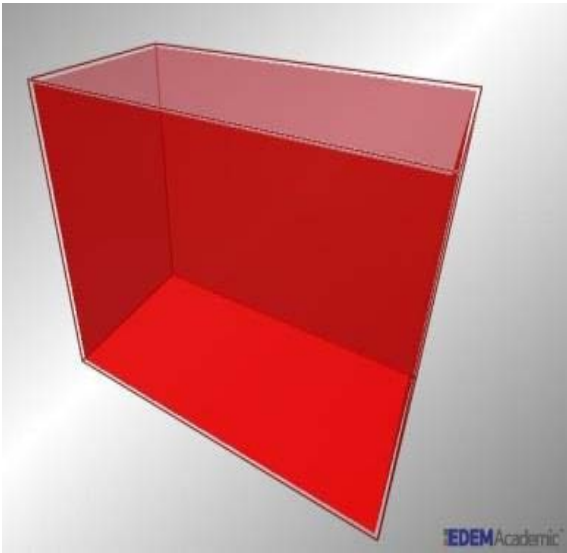

Figure 3. Remodeled soil particle.

Figure 4. Empty virtual box.

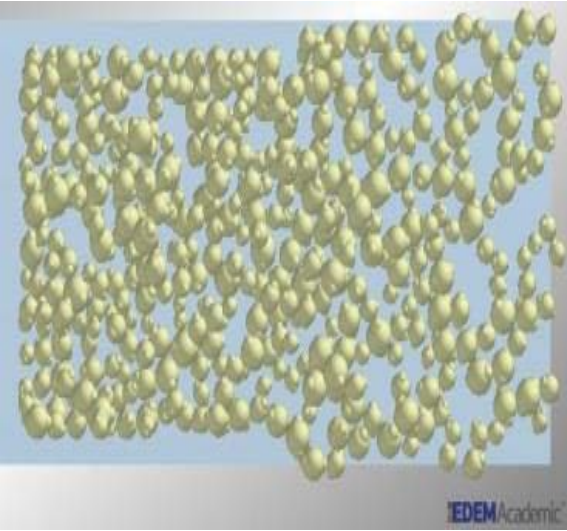**Figure 5.** Particles dropping from the particle factory.
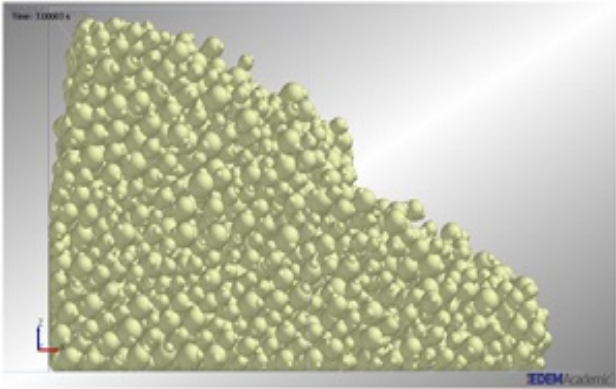

Figure 6. Slumped soil mass in EDEM showing the angle of repose.

2.3. Experimental

Verifications of the simulated results was carried out through experimental work and calculating the total draught force as per the Saunders Equation as explained below.

Saunders Equation

[5] [21] outlined the basis of this model. The model predicts draught force in a semi-rigorous manner. The equation calculated the draught force as a sum of all the forces acting on the plough point, the plough share, the force due to the mouldboard soil momentum change, increase in soil potential energy, friction forces and the lateral forces at the share, mouldboard and that due to the soil lateral movement. It considered soil parameters and plough geometric factors. **Figure 7** is a diagrammatical representation of the different components attributing to the total draught force.

Equation (3) is quadratic equation that shows the relation between draft, speed, plough design characteristics and the soil conditions according to [5] [13].

$$H_t = H_p + H_s + H_{mc} + H_e + H_{cs} + H_{ms} + H_{fs} \tag{3}$$

where:

H_t is the total draught force in KN.

H_p is the draught force due to plough point.

H_s is the draught force due to plough share.

H_{mc} is the draught force due to mouldboard soil momentum change and draught force friction along the mouldboard.

H_e is the draught force due to the increase in soil potential energy and the mouldboard

H_{cs} and H_{ms} are the draught force arising from friction forces due to lateral forces at the share and at the mouldboard.

H_{fs} is the draught force arising from lateral forces at the mouldboard because of the lateral soil movements.

The above model aims at predicting the total plough draught forces in a semi rigorous manner. The constituents of Equation (3) were further broken down as shown in Equations (4)-(9).

$$H_p = \left(\gamma d_p^2 N_r C d_p N_{ca} \right) w_p 0.55 d_p \left(m - \right) \left(\frac{\gamma v^2 N_a d_p}{g} \right) \left(w_p 0.33 d_p \right) \sin \left(\propto_p \sigma \right) \tag{4}$$

$$H_s = \left(\gamma d_s^2 N_r + C d_s N_{ca} \right) + \left(\frac{\gamma v^2 N_{ad_p}}{g} \right) [W_s] \sin \left(\propto_p + \sigma \right) \sin \beta \tag{5}$$
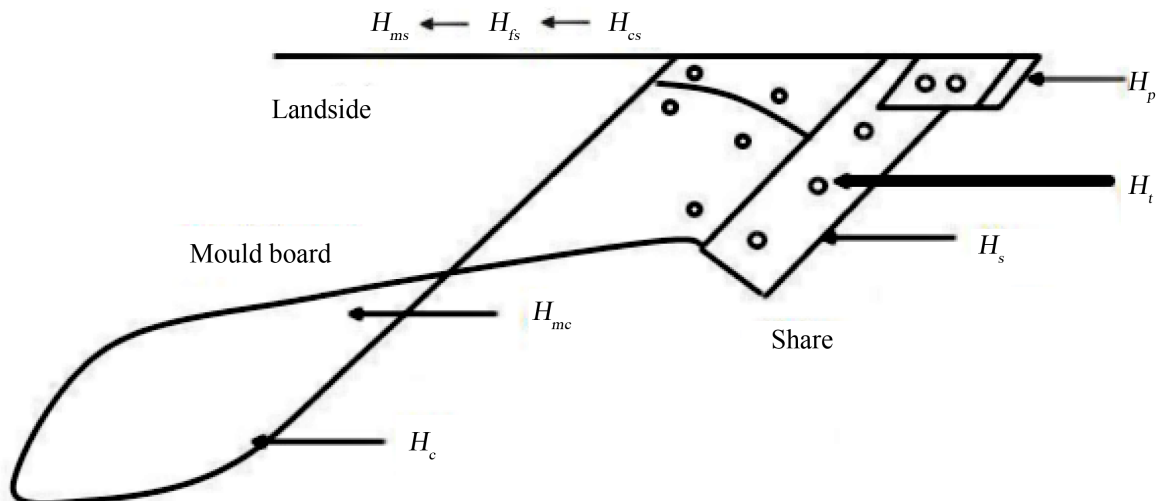

Figure 7. Diagram of the components of the draught force acting on the plough.

$$H_{mc} = \left(\frac{\gamma}{g}\right)\left(w_p d_p + w_s d_s\right)v^2\left[1 - \{1 - \sin\theta \tan\sigma\}\cos\theta\right] \tag{6}$$

$$H_e = (2\gamma)\left(w_p d_p + w_s d_s\right)d_s \tag{7}$$

$$H_{cs} = \left[\left(\gamma d_s^2 N_r + Cd_s N_{ca}\right) + \left(\frac{\gamma v^2 N_{ad_s}}{g}\right)\right]w_s \sin\left(\propto_s + \sigma\right)\cos\beta \tan\sigma \tag{8}$$

$$H_{ms} = \left(\frac{\gamma}{g}\right)\left(w_p d_p + w_s d_s\right)v^2\left[\sin\theta - \{1 - \sin\theta \tan\sigma\}\tan\theta\right] \tag{9}$$

3. Results and Discussion

EDEM simulation was performed by conducting iterations for each variable of frog angle, cutting depth and speed on the same type of soil. A VBA was developed and used to perform the rigorous mathematical Saunders equation. All the results were transferred to excel sheets for smoothening.

Sandy Clay soil was used and the soil parameters as determined by the shear test are outlined in **Table 2**.

Table 3 shows the parameters of the mould plough used. The mouldboard had only one plough.

The soil type was not varied. However, the speed, depth and frog angle varied as shown in **Table 4**.

The EDEM simulated total draught force results compared ± 15.95% to those determined through Saunders Equation.

3.1. Effect of Speed on Draught Force

The draught force increased as the speed increased. The relationship between draught force and speed was seen as 2nd degree polynomial quadratic equation.

Table 2. Soil parameters.

Bulk unit weight (KN/m³)	18
Cohesion (KN/m²)	78
Shearing resistance angle	38°
Soil metal friction angle	20°
Soil soil friction angle	0.7813[*]

[*]Soil soil friction angle was determined as Tan of the shearing resistance angle.

Table 3. Plough Geometric parameters.

Plough angle	25°
Share rake angle	20°
Mouldboard angle to the direction of motion	155°
Share edge angle to the direction of motion	26°
Width of the plough (m)	0.26
Mouldboard length (m)	0.72

Table 4. Assumed operating conditions for optimization.

Depth of tillage (m)	**0.1 - 0.3[*]**
Speed of tillage (m/s)	**1.0 - 4.0[**]**
Frog Angle	30° - 50°[***]

[*]The depth of tillage was varied from 0.1 to 0.3 m with intervals of 0.1 m per range. [**]The speed of tillage was broadly divided into low speeds (≤2.5 m/s) and high speeds (2.5 m/s > 5 m/s). [***]The frog angles used were 30°, 40° and 50°.

Figure 8 shows the behavior of draught force determined by EDEM simulation across all the frogs. Draught force increased as speed increased for frog 30˚ and 40˚. For frog 50˚ the draught force increased slightly and only picked at speeds higher than 4 m/s showing a more stable relationship with increase in speed.

Figure 9 shows the behavior of draught force determined by Saunders Equation across all the frogs. Draught force increased as speed increased across all the frog angles. At speeds above 3.25 m/s there was an increase of draught force of about 45.8% per each increase of 0.5 m/s of speed.

As the speed increased across the frog angles used, the draught force increased. The optimum speed of operation according to the results was 1.6 m/s which was agreeable with the various literature materials [8] [13] [15].

3.2. Effect of Cutting Depth to Draught Force

As the depth increased the draught force also increased linearly. **Figure 10** and **Figure 11** are of draught force determined through Simulation (EDEM), and Saunders equation Vs. Depth of tillage respectively. The draught force in the graphs is of the three depths: 8 cm, 16.25 cm and 24.25 cm they show how draught force increase linearly as depth of tillage increases.

The two methods used to determine the draught force showed a linear relationship between the draught force and the depth. The depth of tillage is a determinant of the crop being planted.

4. Conclusions

A mathematical model (Saunders Equation) of a mouldboard was used to describe the draught force with emphasis on the different forces acting on the mouldboard parts contributing to the total draught force. DEM model was used to simulate the tillage process in a controlled environment. The simulations were iterated to achieve
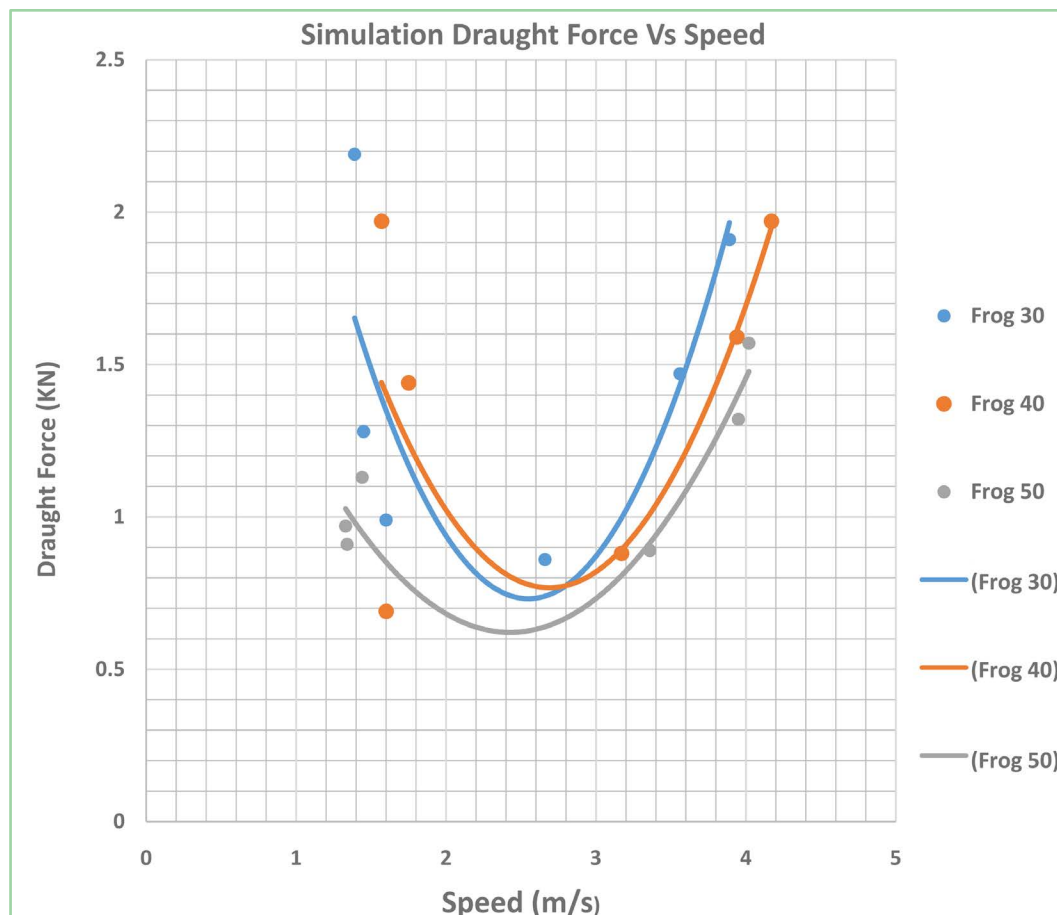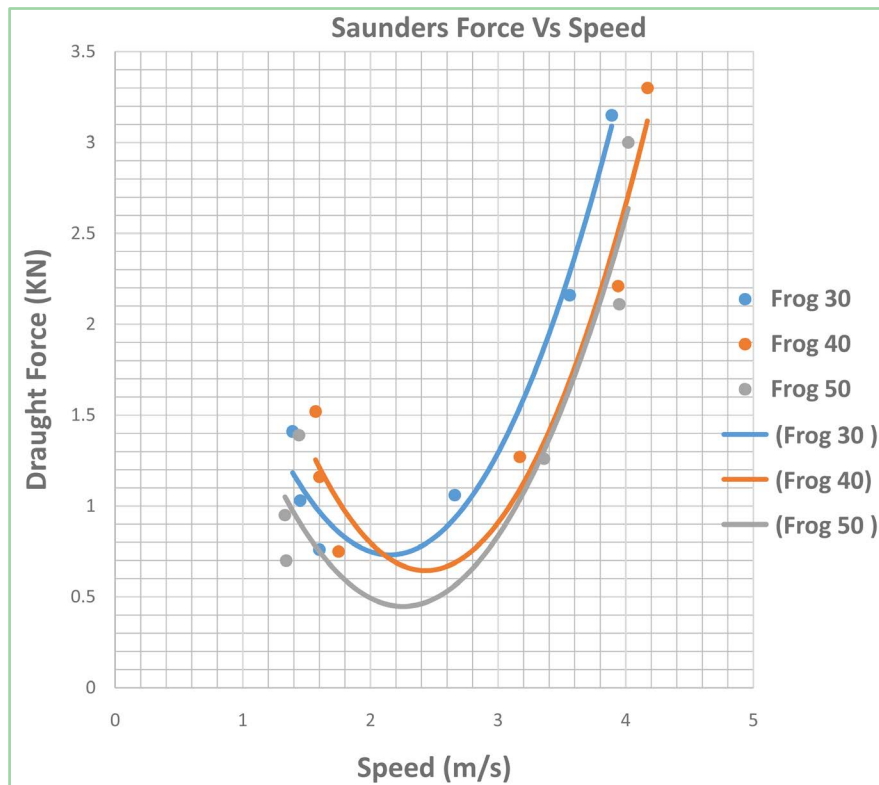

Figure 8. Simulation draught force vs speed.

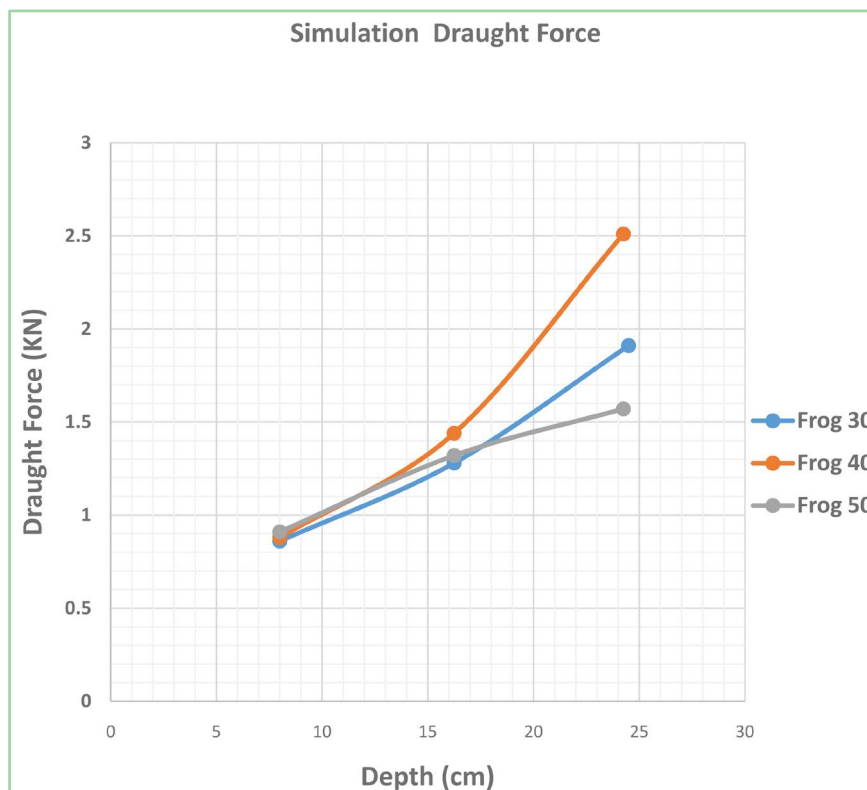**Figure 9.** Draught force vs speed.

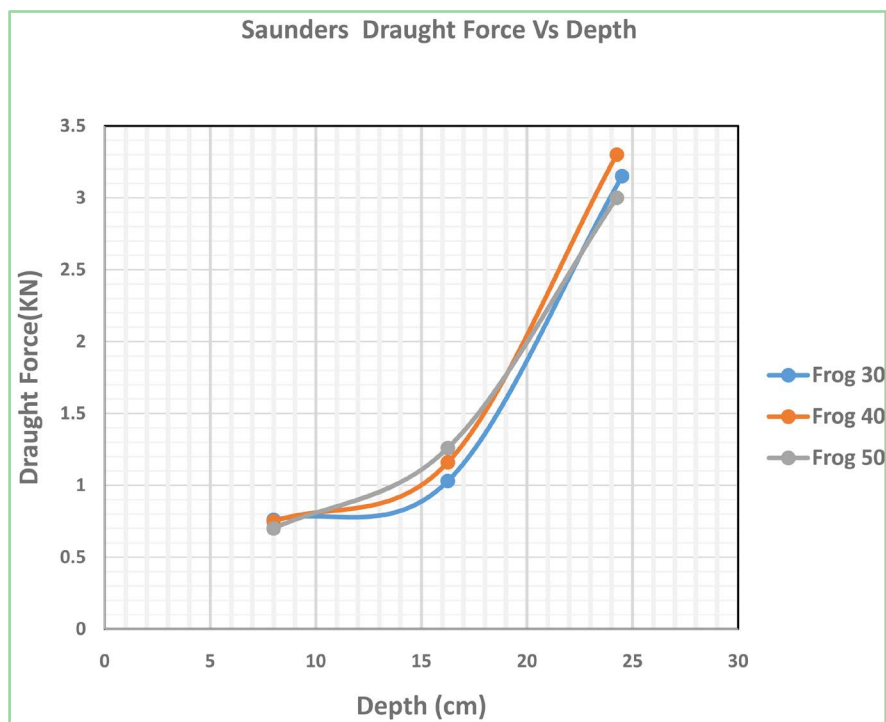**Figure 10.** Simulation draught force vs depth.

Figure 11. Saunders equation draught force vs depth.

the optimal operating parameters of the plough. The draught forces determined by the Saunders Equation were verified through DEM simulation showing a variance of ±0.15.

Statistical analyses of the draught forces determined by the two methods showed there was minimal significant difference between the measured and simulated data. It was observed that the mouldboard required more draught force at higher speeds and cutting depth. At higher speeds the Saunders Equation was not able to describe draught force as reliably.

The results determined that DEM is an effective tool of determining draught force as it is fast and reliable. 30˚ frog angle was the optimum angle at a speed of 1.6 m/s. DEM predicted draught forces at this angle was in good agreement with the measured values with an error range of 7.6% to 14.5% for a speed range of 1.5 m/s to 1.8 m/s.

Acknowledgements

References

[1]   Formato, A. Faugno, S. and Paolillo, G. (2005) Numerical Simulation of Soil Plough Mouldboard Interaction. *Biosystems Engineering*, **92**, 309-316. http://dx.doi.org/10.1016/j.biosystemseng.2005.07.005

[2]   Kushwaha, R.L. and Zhang, J. (1998) Dynamic Analysis of a Tillage Tool Part 1—Finite Element Model. *Canada Agricultural Engineering*, **40**, 287-292.

[3]   Owend, P.M.O. and Edward, S.M. (1996) Characteristic Loading of Light Mouldboard Ploughs at Low Speeds. *Journal of Terramechanics*, **335**, 29-53. http://dx.doi.org/10.1016/0022-4898(96)00011-0

[4]   Shrestha, D.S., Sing, G. and Gebresenbet, G. (2001) Optimizing Design Parameters of a Mouldboard Plough. *Journal of Agricultural Engineering Research*, **78**, 377-389. http://dx.doi.org/10.1006/jaer.2000.0663

[5]   Godwin, R.J., O' Dogherty, M.J., Saunders, C. and Balafoutis, A.T. (2007) A Force Prediction Model for Mouldboard Plough Incorporating the Effects of Soil Characteristics Properties, Plough Geometric Factors and Ploughing Speed. *Biosystem Engineering*, **97**, 117-129. http://dx.doi.org/10.1016/j.biosystemseng.2007.02.001

[6]   Bentaher, H., Ibrahim, A., Hamza, E., Hbaieb, M., Kantchev, G., Malley, A. and Arnold, W. (2013) Finite Element Modelling Simulation of Mouldboard Plough Soil Interaction. *Soil and Tillage Research*, **134**, 11-16. http://dx.doi.org/10.1016/j.still.2013.07.002

[7]   Temesgen, M. Savenije, H.H., Rockstorm, J. and Hoogmad, W.B. (2012) Assessment of Strip Tillage Systems on Maize Production in Semi-Arid Ethiopia. *Physics and Chemistry of Earth Parts A/B/C*, **47-48**, 156-165. http://dx.doi.org/10.1016/j.pce.2011.07.046

[8]   Zadeh, S.R. (2006) Modelling of Energy Requirement by a Narrow Tillage Tool (PhD). University of Saskatchewan, Saskatoon, p. 190.

[9]   Mckeys, E. (1985) Soil Cutting Tillage. Elsevier, Amsterdam.

[10] Martin, O., Klaus, D., Christos, V. and Peter, E. (2011) Prediction of Draft Forces in Cohesionless Soil with the Discrete Element Method. *Journal of Terramechanics*, **48**, 347-358.

[11] Oida, A. and Momozu, M. (2002) Simulation of Soil Behavior and Reaction by Machine Part by Means of DEM. *Agricultural Engineering International*: *The CIGR EJournal*, **IV**, 1-7.

[12] Cundall, P.A. and Strack, Q.D.L. (1971) A Discrete Numerical Model for Granular Assemblies. *Geotechnique*, **29**, 47-65.

[13] Owen, D.R.J., Feng, Y.T., De Souza Neto, E.A., *et al.* (2004) The Modelling of Multi Fracture Solids and Particulate Media. *International Journal for Numerical Methods in Engineering*, **60**, 317-339.

[14] Nezami, E.G., Hashash, Y.M.A., Zhao, D. and Ghaboussi, J. (2007) Simulation of Front end Loader Bucket-Soil Interaction Using Discrete Element Model. *International Journal for Numerical and Analytical Methods in Geomechanics*, **31**, 47-62.

[15] Coetzee, C. and Els, D. (2009) The Numerical Modelling of Excavator Bucket Filling Using DEM. *Journal of Terramechanics*, **46**, 217-227.

[16] Coetzee, C., Els, D. and Dymond, G. (2010) Discrete Element Parameter Calibration and the Modelling of Dragline Bucket Filling. *Journal of Terramechanics*, **47**, 33-44.

[17] Mustafa, U., John, F. and Chris, S. (2014) Three Dimensional Discrete Element Modelling of Tillage: Determination of a Suitable Contact Model and Parameters for a Cohesionless Soil. *Biosystem Engineering*, **10**, 106-117.

[18] Ucgul, M., Fielke, J.M. and Saunders, C. (2015) Defining the Effect of Sweep Tillage Tool Cutting Edge Geometry on Tillage Forces Using 3D Discrete Element Modelling. *Information Processing in Agriculture*, **2**, 130-141.

[19] Raji, A.O. (1999) Discrete Element Modelling of the Deformation of Bulk Agricultural Particles (PhD). University of Newcastle, Newcastle, p. 165.

[20] EDEM (2010) EDEM User Guide. DEM Solutions, Edinburgh. www.dem-solutions.com

[21] Saunders, C., Godwin, R.J. and O'Dohgerty, M.J. (2000) Prediction of Soil Forces Acting on Mouldboard Plough. Fourth International Conference on Soil Dynamics, Adelaide.